Indian Journal of Chemistry
Vol. 65, March 2026, pp. 264-269
DOI: 10.56042/ijc.v65i3.24514

Density functional theoretical study and DNA cleavage activity of 2,5-bis (cyclohexylamino)cyclohexa-2,5-diene-1,4-dione

A Asha* & Antony Bruz

Department of Chemistry, BJM Government College, Chavara, Kollam 691 583, Kerala, India
E-mail: ashaapillai@gmail.com

Received 5 October 2025; accepted (revised) 9 March 2026

Herein is reported the density functional theoretical study and DNA cleavage activity of an aminobenzoquinone, 2,5-bis(cyclohexylamino)cyclohexa-2,5-diene-1,4-dione (BCBQ). Despite aminobenzoquinones being recognized for their biological activity, they remain relatively unexplored in theoretical studies. Single crystal X-ray analysis of BCBQ has already been reported. Detailed analysis of its structural parameters has elucidated the biological activity of such compounds, aiding the design of substituted ABQs for multiple uses.

Keywords: Aminobenzoquinones, DFT study, DNA cleavage activity

Biological electron transfer processes including cellular respiration and photosynthesis manifests the inevitable role played by *p*-benzoquinones and their amino derivatives[1,2]. They are widespread in many fungi which are the colour bearing pigments in them[3]. Use of Mitomycin as an anti-cancer and anti-bacterial agents is well demonstrated in the literature[4]. The anti-bacterial as well as the anti-fungal activity of aminobenzoquinones has been studied extensively which points their significance in pharmacology[5,6]. Benzoquinones and related compounds are effective redox reagents able to generate reactive oxygen species (ROS) which acts as electrophiles forming covalent bonds with tissue nucleophiles[7].

The vibrational spectra of amino naphthoquinones were studied by various research groups[8], however 2,5-diamino1,4-benzoquinones are less explored. This lead us to focus on the DFT study and DNA cleavage activity study of synthesized BCBQ.

Experimental Section

Materials

Cyclohexylamine and ethyl vanillin were of A R grade purchased from Merck and were used without any purification. Solvents used were purchased from Merck and used as received.

Synthesis of 2,5-bis(cyclohexylamino)cyclohexa-2,5-diene-1,4-dione

BCBQ was synthesized by the previously reported method[9]. Ethyl vanillin (10 mmol) and cyclohexylamine (20 mmol) were mixed in 20 mL methanol along with addition of a trace amount of glacial acetic acid and allowed for slow evaporation under open air at RT. Complete evaporation of methanol resulted in red needle shaped crystals of BCBQ. m.p.240-241°C. IR (KBr): 3270, 2852, 1640, 1562, 1091 cm^{-1}; UV-Vis λ_{max} (MeOH) nm: 306, 395, 453; ^{1}H NMR ($CDCl_3$): δ 1.18–1.42 (m, 10H), 1.59–1.69 (m, 3H), 1.74–1.83 (m, 4H), 1.94–2.02 (m, 4H), 3.26 (m, 2H), 5.33 (s, 2H), 6.59 (d, *J* ¼ 9 Hz, 2H); ^{13}C NMR ($CDCl_3$): δ 24.5, 25.4,31.8, 51.3, 92.8, 150.2, 178.1; HR-ESI-MS: *m/z* Calcd for $C_{18}H_{27}N_2O_2$ [M^+H^+]: 303.2073. Obsd: 303.2078.

DFT study

The quantum chemical calculations have been carried out by DFT method using the Gaussian '09 software[10] by using B3LYP functional, employing 6-311 ++G(d,p) basis set which is the most effective level of theory, available for the analysis of metallic systems[11]. The computed optimized geometry, IR and Raman spectra, Eigen vector distribution of vibrational modes, obtained using Gauss view 5.0 program[12] and PED[13] have been used for the comprehensive molecular structural and vibrational analysis. The calculated vibrational frequencies have been scaled, using standard scaling factor 0.9671 (Ref. 14).

In vitro DNA cleavage assay

Bacterial cultures were grown in LB medium with appropriate antibiotics at 37°C and kept overnight (O/N) with shaking. The O/N culture was transferred

to a 1.5 mL eppendorf tube, and spun down cell culture (twice) at high speed for 1 min at table-top centrifuge. The supernatant was discarded. To the pellet 100 µL of resuspension solution (P1 buffer) was added into each tube and vortexed to completely resuspend the cell pellet. After that 100 µL of lysis solution (P2 buffer) was added and mixed gently by inverting the tube 5-6 times. The solution should quickly turn transparent and become more viscous indicating bacterial lysis has taken place. Then 150 µL of neutralizing solution (P3 buffer) was added and mixed thoroughly by inverting the tubes several times. At this point bacterial chromosomal DNA is usually seen as a white precipitate.

The tubes were centrifuged at high speed for 10 min and transferred the supernatant (try to not disturb the white precipitate) carefully to a new labeled 1.5 mL eppendorf tube with a 1 mL pipette. To the supernatant 2.5-3 volume of 80% of cold ethanol (stores at –20°C) to each tube was added and mixed gently by inverting the tubes a few times. Then the plasmid DNA precipitate was centrifuged (transparency pellet) at high speed for 10 min. the supernatant was discarded and removed the remaining liquid as much as possible by leaving the tube upside-down on a piece of paper towel, then kept the tubes in a tube holder and air dried for 10-20 min. To dry faster, keep tubes at 37°C heat blocker. DNA precipitate turns white when dry.

The DNA pellet was resuspended with 50 µL TE buffer and dissolved completely by pipetting solution several times. To the resuspended pellet RNAse 10 µg/mL was added and incubated at 37°C for 1 hr. After incubation 250 µL of chlorofom and isoamyl alcohol (24:1) was added. To this mixture 250 µL of phenol saturated with tris was added. Centrifuged at 13000 rpm for 5 min. The aqueous layer was carefully transferred to an clean and sterile eppendorf tube and 50 µL of 1M NaCl was added. After that 1 mL of ethanol was added and kept overnight at –20°C for ethanol precipitation. After the incubation period it was centrifuged at 13000 rpm for 15 min. The pellet was washed in 70% ethanol, centrifuges, air dried the pellet and resuspended in TE under aseptic condition (Laminar Air Flow Chamber).

In vitro DNA damage protection assay

Plasmid DNA nicking assay was performed using pUC 18 plasmid DNA as per the method[15]. A mixture of 10µL of extract (10µg) and plasmid DNA (10µL) was incubated at RT for 30 min at 37°C. A tube with plasmid was kept as negative control and one with 10µL of Fenton's reagent (30 mM H_2O_2, 50 mM ascorbic acid and 50 mM $FeCl_3$) as positive control. The DNA samples were electrophoresed on 1% agarose gel.

Agarose gel electrophoresis

Agarose gel electrophoresis is a method for separating and visualizing DNA fragments. The fragments are separated by charge and size and move through agarose gel matrix, when subjected to an electric field. The electric field is generated by applying potential across an electrolyte solution (buffer).When boiled in an aqueous buffer, agardissolve and upon cooling solidifies to a gel. 1.5% agarose gel was prepared in 1×TE buffer and melted in hot water bath at 90°C.Then the melted agarose was cooled down to 45°C. 6µL of 10 mg/mL of ethidium bromide was added and poured in to gel casting apparatus with the gel comb. After setting, the comb was removed from the gel. The electrophoresis buffer was poured in the gel tank and the platform with the gel was placed in it so as to immerse the gel.The gel was loaded with the samples and run at 50 V for 30 min. The stained gel was visualized using a gel documentation system (E gel imager, Invitrogen)[16].

Results and Discussion

DFT study

Density functional studies has been carried out for structure and vibrational spectra of transient intermediates of *p*-benzoquinone[17]. Nonella *et al*. has studied the IR spectrum of *p*-benzoquinone in water obtained from QM/MM hybrid molecular dynamic simulation[18]. The correlation graphs between experimental and computational wavenumbers of IR and Raman spectra are shown in Fig. 1. The graph shows a good agreement between experimental and scaled wavenumbers calculated by DFT/B3LYP/ 6-311 ++G (d, p) method mostly in the finger print region. The optimized molecular structure of BCBQ is shown in Fig. 2.

In P-benzoquinone, the typical C═O bond length is 1.225Å (Ref. 19) whereas in BCBQ, this bond lengthens to 1.235Å due to the electron-donating amino substituent at the *ortho* position, which is in direct conjugation with the carbonyl group. Both theoretical and experimental data align, showing the

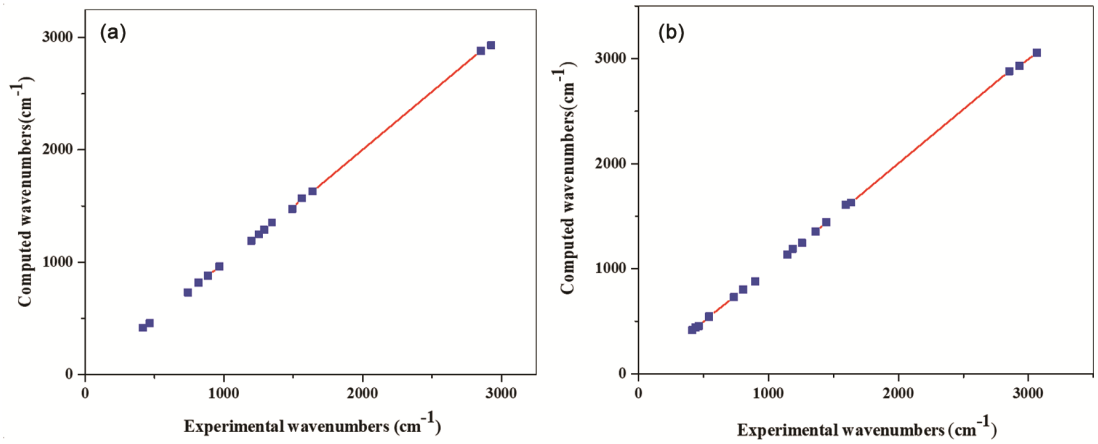

Fig. 1 — correlation graphs between experimental and computational wavenumbers of IR (left) and Raman spectra (right) in BCBQ

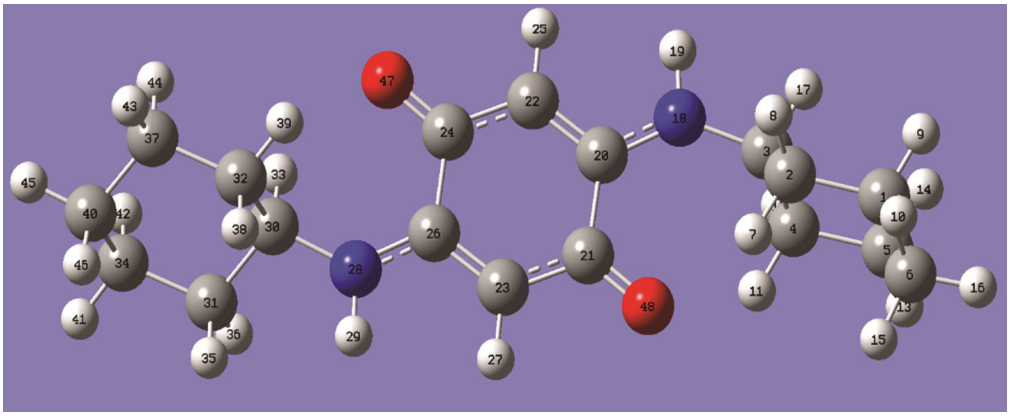

Fig. 2 — Optimized molecular structure of BCBQ calculated using DFT at the B3LYP/6-311 ++G (d, p) level

C═O (symm) stretching frequency as a medium-intensity band at 1640 cm^{-1} in the IR spectrum and 1637 cm^{-1} in the Raman spectrum. The calculated C═O (symm) stretching frequency is 1630 cm^{-1}. This discrepancy can be attributed to the presence of intermolecular and intramolecular hydrogen bonding involving the carbonyl group in solid-state BCBQ crystals, which isn't present in the gaseous phase. The C═O (antisymm) stretching mode shows a very strong band at 1593 cm^{-1} in Raman, is IR-inactive, and correlates with the calculated frequency at 1608 cm^{-1}. Significant deviations from unsubstituted PBQ are seen in these values, emphasizing the impact of electron-releasing amino groups in *ortho* positions, consistent with the observed bond lengths. Because of conjugation between the nitrogen lone pair and the carbonyl group, the bond lengths of C(21)-C(23) and C(22)-C(24) are shorter (1.413Å and 1.410Å) than in unsubstituted PBQ (1.481Å). The C=C (symm) stretching frequency shows a substantial decrease from 1616 cm^{-1} to 1493 cm^{-1} as a result of π-electron conjugation. Theoretical and experimental C-C (antisymm) stretching frequencies (1569 and 1563 cm^{-1}) show strong correlation and a notable difference compared to the unsubstituted counterpart (1592 cm^{-1}). Inter- and intramolecular hydrogen bonding occurs between NH and the carbonyl group in BCBQ's crystal lattice. This network of hydrogen bonds results in a considerable difference between experimental and theoretical N-H stretching frequencies. The N-H stretch appears at 3271 cm^{-1} in IR and 3272 cm^{-1} in Raman experimentally, differing substantially from the calculated 3449 cm^{-1} because gas-phase calculations don't account for hydrogen bonding. Further evidence comes from bond length data: theoretically predicted values (1.01Å) show a shortening in BCBQ in the solid state (0.86Å). The C-H stretching vibration in the benzoquinone ring is close to the computational value (3057 cm^{-1}) at 3066 cm^{-1}, while the predicted bond length (1.085Å) is

slightly longer than the experimental value (0.93Å), reflecting the overall effect of conjugation.

For the cyclohexylamino substituents, all C-C bond lengths are shorter than the calculated values. The C-H stretching frequency of the cyclohexyl ring (2927 cm^{-1} in IR, 2931 cm^{-1} in Raman) correlates closely with the calculated value (2931 cm^{-1}), with bond lengths slightly shortened (0.97Å). A similar trend is observable in bending vibrations as well. BCBQ shows an overall reduction in bond lengths and bond angles, mainly due to conjugation with the electron-donating amino group. Calculated and experimental infrared and Raman frequencies along with assignments are given in Table 1. The experimental and theoretical bond lengths and the corresponding assignments are given in Table 2.

In vitro DNA cleavage assay

Gel electrophoresis is a widely using technique for the study of binding of organic and inorganic compounds with nucleic acids[20]. The molecular segregation occurs on the basis of their relative rate of movement through a gel under the influence of an electric field.

Agarose Gel Electrophoresis

Gel electrophoresis images shown in Fig. 3 shows differences in band width and ethidium-bromide staining intensities compared to the control. The capacity of BCBQ to bind or cleave plasmid DNA can be determined by examining differences in band width and intensity. Fig. 3 depicts bands with different widths and brightness relative to the control, implying significant binding/cleavage of DNA by BCBQ as compared to the control where DNA intensity is more pronounced. A single, intense band, close to the top of the gel indicate intact, supercoiled or circular plasmid DNA. BCBQ shows much fainter band at the same position as the control. Faint additional bands are visible below the main band which indicate its DNA cleavage activity. Since lower molecular weight fragments migrate further down, it indicates that Some DNA has been fragmented. Lower band intensity compared to control shows that the original intact DNA is reduced. The reduced intensity of the intact band and the presence of smearing/faint lower bands indicate that the DNA is being cut into smaller pieces.

Table 1 — Calculated vibrational wavenumbers (scaled), measured Infrared and Raman band positions and assignments

FTIR Frequency (cm^{-1})	FTIR Relative Intensity	FTRAMAN Frequency (cm^{-1})	FTRAMAN Relative Intensity	Computed Scaled (cm^{-1})	Assignment
3271	vvs	3272	vw	3449	ν N–H (100)
—	—	3066	vw	3057	ν (C–H) BQ (91)
2927	s	2931	w	2931	ν (C–H) CHA rt (66)
2852	m	2852	m	2881	ν (C–H) CHA lft (89)
1640	m	1637	m	1630	ν (C=O) (69)
—	—	1593	vvs	1608	ν (C=O) (72)
1563	vs	—	—	1569	ν (C–C)(38) + δ (HNC)(24)
1493	s	—	—	1473	ν (C=C) BQ (8)
—	—	1444	w	1442	δ (HCH) CHA rt (75)
1347	s	1362	vw	1353	δ (HCC) CHA lft (28)
1289	s	—	—	1288	τ (HCNC) CHA (19) + τ (HCCC) CHA(10)
1252	m	1257	vw	1247	δ (HCC) CHA rt (22) + τ (HCCC) CHA (26)
1198	w	1184	vw	1190	δ (HCC) BQ(59)
—	—	1143	vw	1133	τ (CCCC) CHA rt(58)
969	m	—	—	960	δ (CCC) (11)
885	w	898	vw	879	ν (C–C) CHA lft (29) + τ (HCCC) CH_2 lft(11)
818	s	—	—	817	δ (HCCN) BQ (70) + OUT (OCCC)(14)
—	—	804	vw	804	δ (CCCQ)(20)
742	m	733	vw	730	δ (HCCN) BQ (17) + OUT (OCCC)(42)+ OUT(NCCC)(23)
—	—	543	vw	546	δ (CCC) (27)
—	—	542	vw	541	τ (HNCC)(68)
467	vw	461	w	455	δ (CCC)(11)+δ (OCC)(11)+δ (CCC)(24)CHA lft
—	—	440	w	442	δ (CCC)(49)CHA lft
417	m	412	w	415	OUT (OCCC)(18)+OUT (NCCC)(34)

Table 2 — Measured and theoretical bond lengths in BCBQ

Parameter	Bond Lengths (Å)		
	Experimental	Theoretical	
C(24)-O(47)	1.235	1.232	
C(21)-O(48)	1.234	1.231	
C(24)-C(26)	1.51	1.524	
C(20)-C(21)	1.506	1.523	
C(23)-C(26)	1.365	1.373	PBQ
C(20)-C(22)	1.364	1.375	ASSIGNMENTS
C(21)-C(23)	1.413	1.432	
C(22)-C(24)	1.41	1.431	
C(23)-H(27)	0.93	1.085	
C(22)-H(25)	0.931	1.085	
C(20)-H(18)	1.333	1.357	
C(26)-H(28)	1.336	1.352	
N(28)-H(29)	0.86	1.009	NH
N(18)-H(19)	0.86	1.012	ASSIGNMENT
N(18)-C(3)	1.456	1.482	$N\text{-}C_{cyclohexyl}$
N(28)-C(30)	1.448	1.472	Assigment
C(30)-C(31)	1.513	1.533	
C(30)-C(32)	1.519	1.539	
C(3)-C(4)	1.508	1.538	
C(3)-C(2)	1.52	1.538	
C(31)-C(34)	1.524	1.536	
C(32)-C(37)	1.519	1.535	-C (cyclohexyl)
C(2)-C(1)	1.516	1.537	ASSIGNMENT
C(4)-C(5)	1.524	1.537	
C(34)-C(40)	1.517	1.535	
C(37)-C(40)	1.516	1.534	
C(1)-C(6)	1.503	1.534	
C(5)-C(6)	1.513	1.534	
C(3)-H(17)	0.98	1.097	$N\text{-}C_{cyclohexyl}$ –H
C(30)-H(33)	0.98	1.088	Assigment
C(32)-H(38)	0.969	1.098	
C(32)-H(39)	0.97	1.092	
C(31)-H(35)	0.97	1.094	
C(31)-H(36)	0.97	1.094	
C(2)-H(7)	0.97	1.09	
C(2)-H(8)	0.97	1.095	C-H (cyclohexyl)
C(4)-H(11)	0.97	1.09	ASSIGNMENT
C(4)-H(12)	0.97	1.095	
C(34)-H(41)	0.97	1.094	
C(34)-H(42)	0.969	1.097	
C(37)-H(43)	0.97	1.094	
C(37)-H(44)	0.97	1.097	
C(5)-H(13)	0.97	1.094	
C(5)-H(14)	0.97	1.098	
C(1)-H(9)	0.97	1.098	
C(1)-H(10)	0.969	1.094	
C(40)-H(45)	0.971	1.094	
C(40)-H(46)	0.97	1.097	
C(6)-H(15)	0.969	1.096	
C(6)-H(16)	0.97	1.094	

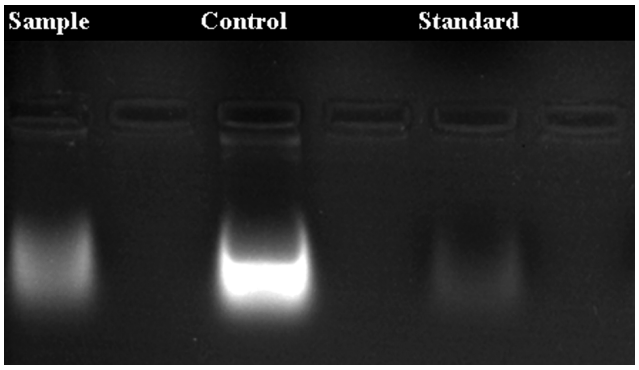

Fig. 3 — Gel electrophoresis images of BCBQ with plasmid DNA

Conclusion

In conclusion, a detailed theoretical investigation on the structure of an aminobenzoquinone BCBQ was carried by DFT study. BCBQ exhibits a general decrease in bond lengths and bond angles, largely attributable to conjugation with the electron-donating amino substituent. H-bonding observed in the BCBQ crystal adequately explains its DNA cleavage activity, as amino groups can facilitate interactions with DNA *via* H-bonding, helping position the quinone moiety near the DNA backbone for effective cleavage.

References

1 Ferreira VF, De Carvalho A S, Ferreira P G, Lima C G & De C D Silva F, *Med Chem*,17 (2021) 1073.
2 Zhang Y, Liu J, Chen X-Q, Chen C-Y, *Food Fun*, 9 (2018) 5653.
3 Park H B, Crawford J M & Lumiquinone A, *J Nat Prod*, 78 (2015) 1437.
4 Shetty R, Kumar N R, Subramani M, Krishna L, Murugeswari P, Matalia H, Khamar P, dadachanji Z V, Mohan R R, Ghosh A & Das D, *Sci Rep*, 11 (2021) 4392.
5 Bayrak N, Yıldız M, Yıldırım H, Mataracı-Kara E & Tuyun A F, *Res Chem Int*, 47 (2021) 2125.
6 Yıldız M, *J Mol Struc*, 1203 (2020) 127422.
7 Dias F R, Guerra F S, Lima F A, Castro Y K D, Ferreira V F, Campos V R, Fernandes P D & Cunha A C, *J Brazilian Chem Soc*, 32 (2021) 476.
8 Jadhav B, Dhawale S, Gadekar B, Ingale S & Deshmukh S, *Int J Chem Sci*, 5 (2021) 6.
9 Asha A, Mohan A S, Suma S, Sudarsanakumar M & Kurup M P, *J Mol Struc*, 1141 (2017) 299.
10 Gaussian 09, Revision D.01, Frisch M, Clemente F, Frisch M J, Trucks G W, Schlegel H B, Scuseria G E, Robb M A, Cheeseman J R, Scalmani G, V Barone, B Mennucci, Petersson G A, Nakatsuji H, Caricato M, Li X, Hratchian H P, Izmaylov A F, Bloino J, Zhe G, Sonnenberg J L, Hada M, Ehara M, Toyota K, Fukuda R, Hasegawa J, Ishida M, Nakajima T, Honda Y, Kitao O, Nakai H, Vreven T, Montgomery J. A, Peralta J J E, Ogliaro F, Bearpark M, Heyd J J, Brothers E, Kudin K N, Staroverov V N, Kobayashi R, Normand J, Raghavachari K, Rendell A, Burant J C, Iyengar S S, Tomasi J, Cossi M, Rega N, Millam

J M, Klene M, Knox J E, Cross J B, Bakken V, Adamo C, Jaramillo J, Gomperts R, Stratmann R. E, Yazyev O, Austin A J, Cammi R, Pomelli C, Ochterski J W, Martin R L, Morokuma K, Zakrzewski V G, Voth G A, Salvador P, Dannenberg J J, Dapprich S, Daniels A D, Farkas Ö, Foresman J B, Ortiz J V, Cioslowski J & Fox D J, (Gaussian, Inc, Wallingford CT), 2009.

11 Kostova I, Peica N & Kiefer W, *Chem Phys*, 327 (2006) 494.

12 Dennington R, Keith T & Millam J, *Semichem Inc. Shawnee Mission KS, GaussView, Version*, 2009.

13 Jamróz M H, Dobrowolski J C & Brzozowski R, *J Mol Struc*, 787 (2006) 172.

14 Andersson M P & Uvdal P, *J Phys Chem A*, 109 (2005) 2937.

15 Harborne J A, *Phytochemical Methods: A Guide to Modern Techniques of Plant Analysis*, (Springer Nature) 1998.

16 Poorna A C, Resmi M S & Soniya E V, *Agricultural Chemistry*, (Intech Open Limited, London, United Kingdom) 2013.

17 Mohandas P & Umapathy S, *J Phys Chem A*, 101 (1997) 4449.

18 Nonella M, Mathias G & Tavan P, *J Phys Chem A*,107 (2003) 8638.

19 Hagen Kr & Hedberg K, *J Chem Phys*, 59 (1973) 158.

20 Xu W, Yang X, Yang L, Jia Z-L, Wei L, Liu F & Lu G-Y, *New J Chem*, 34 (2010) 2654.